



Faculty of Electrical Engineering

**THE CONSTANT SWITCHING FREQUENCY AND TORQUE
RIPPLE REDUCTION OF DIRECT TORQUE CONTROLLED
INDUCTION MACHINE WITH NEUTRAL POINT CLAMPED
INVERTER**

Huzainirah binti Ismail

Master of Science in Electrical Engineering

2018

**THE CONSTANT SWITCHING FREQUENCY AND TORQUE RIPPLE
REDUCTION OF DIRECT TORQUE CONTROLLED INDUCTION MACHINE
WITH NEUTRAL POINT CLAMPED INVERTER**

HUZAINIRAH BINTI ISMAIL

**A thesis submitted
in fulfillment of the requirements for the degree of Master of Science
in Electrical Engineering**

Faculty of Electrical Engineering

UNIVERSITI TEKNIKAL MALAYSIA MELAKA

2018

DECLARATION

I declare that this thesis entitled “The Constant Switching Frequency and Torque Ripple Reduction of Direct Torque Controlled Induction Machine with Neutral Point Clamped Inverter” is the result of my own research except as cited in the references. The thesis has not been accepted for any degree and is not concurrently submitted in candidature of any other degree.

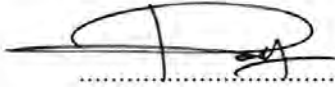
Signature : 

Name : HUZAINIRAH BINTI ISMAIL

Date : 12 / 11 / 2018

APPROVAL

I hereby declare that I have read this thesis and in my opinion this thesis is sufficient in terms of scope and quality for the award of Master of Science in Electrical Engineering.

Signature	:	
Supervisor Name	:	DR FAZLLI BIN PATKAR
Date	:	12/11/2018

DEDICATION

To:

My inspiring parents,

Ismail bin Bujang and Azizah binti Salleh.

My beloved husband,

Azim bin Md Kasim.

My lovely siblings,

Hawa, Haikal, Hafiszullah, Hurmazan, Haziq, Hazim and Hamizah.

For their love, sacrifice, endless support and encouragement to complete this research.

ABSTRACT

Direct Torque Control (DTC) of induction motor drives are widely accepted in variable speed drive applications because it offers high performance in terms of fast torque response as well as simplicity of control structure. However, conventional DTC drives which utilize two-level inverter and hysteresis controllers inherently suffer from two major drawbacks which are large torque ripple and variable switching frequency particularly at low speed operation. This is because the torque is unable to restricted within the hysteresis band (commonly happened in digital implementation of hysteresis controller) that leads to condition of overshoot and undershoot which result in large torque ripple. Secondly, inappropriate selection of voltage vectors for different speed operation as two-level inverter provides only limited numbers of voltage vectors. This research aims to improve the performance of the DTC drives by utilizing a three-level Neutral Point Clamped (NPC) inverter as appropriate voltage vectors can be utilized for different speed operations due to availability of larger number of voltage vectors. Nevertheless, the utilisation of NPC inverter lead to imbalance of upper and lower capacitor voltage due to application of short amplitude of voltage vectors which have two redundant switching states and each switching state produces different effect towards the capacitor voltage. Therefore, a simple capacitor voltage balancing strategy is also proposed to select the appropriate switching states based on capacitor voltage status. Next, the selection of appropriate voltage vectors according to speed operation are determined to produce reduction of torque ripple and switching frequency. Furthermore, a constant switching frequency operation is obtained by replacing the hysteresis torque controller with constant switching frequency (CSF) torque controller. The proposed improvement method was conducted experimentally using DTC-NPC inverter drives with CSF torque controller (with acronym DTC-NPC-CSF) and was compared with conventional DTC drives as well as DTC drives with NPC inverter and hysteresis torque controller (with acronym DTC-NPC-HTC) for performance analysis. The performance result showed that the torque ripple was minimized and the switching frequency was remained constant for all range of speeds.

ABSTRAK

Kawalan dayakilas langsung (DTC) bagi pemacu motor induksi telah diterima secara meluas dalam aplikasi pemacu laju berubah-ubah kerana ia menawarkan prestasi tinggi dari segi kawalan dayakilas yang cepat serta struktur kawalan yang ringkas. Walau bagaimanapun, DTC konvensional yang menggunakan sebuah penyongsang dua peringkat dan pengawal histerisis sememangnya mengalami dua kekurangan yang utama iaitu riak dayakilas yang besar dan frekuensi pensuisan berubah-ubah terutamanya pada operasi kelajuan yang rendah. Kekurangan ini disebabkan oleh dayakilas tidak dapat dihadkan dalam jalur histeresis (kebiasaannya berlaku dalam implementasi pengendali histerisis secara digital) yang menyebabkan keadaan dayakilas yang terlajak naik dan turun sehingga menghasilkan riak dayakilas yang besar. Selain itu, pemilihan vektor voltan yang tidak sesuai untuk keadaan operasi kelajuan yang berlainan kerana penyongsang dua peringkat menyediakan bilangan vektor voltan yang terhad. Kajian ini bertujuan untuk meningkatkan prestasi pemacu DTC dengan menggunakan penyongsang Apitan Titik Neutral (NPC) tiga peringkat di mana vektor voltan yang sesuai dapat digunakan untuk operasi kelajuan yang berbeza-beza kerana terdapat hilangan vektor voltan yang lebih banyak. Walau bagaimanapun, penggunaan penyongsang NPC menyebabkan ketidakseimbangan voltan atas dan bawah kapasitor disebabkan oleh penggunaan vektor voltan beramplitud pendek yang mempunyai dua keadaan pensuisan berulang dan setiap keadaan pensuisan menghasilkan kesan yang berbeza ke atas voltan kapasitor. Oleh itu, strategi pengimbang voltan kapasitor yang mudah juga dicadangkan untuk memilih keadaan pensuisan yang sesuai mengikut keadaan voltan kapasitor. Seterusnya, pemilihan vektor voltan yang sesuai mengikut operasi kelajuan ditentukan supaya dapat menghasilkan dayakilas dan frekuensi pensuisan yang minimum. Selain itu, operasi frekuensi pensuisan yang tetap diperolehi dengan menggantikan pengawal histerisis dayakilas dengan pengawal dayakilas frekuensi pensuisan tetap (CSF). Kaedah penambahbaikan yang dicadangkan dijalankan secara eksperimen menggunakan pemacu penyongsang DTC-NPC dengan pengawal dayakilas CSF (dengan singkatan DTC-NPC-CSF) dan dibandingkan dengan pemacu DTC konvensional serta pemacu DTC dengan penyongsang NPC dan pengawal histerisis dayakilas (dengan singkatan DTC-NPC-HTC) untuk menganalisis prestasi. Keputusan prestasi menunjukkan bahawa riak dayakilas dapat diminimumkan dan frekuensi pensuisan kekal untuk tetap bagi semua julat kelajuan.

ACKNOWLEDGEMENTS

First and foremost, I am grateful to Allah s.w.t for giving me chance and strength to complete this research. Nothing can be done except by the permission of Allah Almighty.

I would like to express my gratitude to my main supervisor, Dr Fazli bin Patkar who gives continuous supervision, guidance and patience during my study especially in completing this thesis.

I am deeply thankful to my co-supervisor which is Dr Auzani bin Jidin for his advice, immense knowledge and provide equipment for experimental works in order to accomplish my master study.

My sincere thanks goes to my colleagues which is Khairi, Faezah, Sundram, Ayu, Lina and Dayah as they always share ideas, understanding, gives encouragement and opinion.

A special thanks and appreciation to my beloved parents and husband that always gives loves, motivation and financial support throughout all my studies. Thank you for staying by my side when I needed the most. Not forgotten my sister Hawa who continuously gives moral support and unending inspiration to finish this study.

TABLE OF CONTENTS

	PAGE
DECLARATION	
APPROVAL	
DEDICATION	
ABSTRACT	i
ABSTRAK	ii
ACKNOWLEDGEMENTS	iii
TABLE OF CONTENTS	iv
LIST OF TABLES	vi
LIST OF FIGURES	viii
LIST OF APPENDICES	xv
LIST OF ABBREVIATIONS	xvi
LIST OF PUBLICATIONS	xx
CHAPTER	
1. INTRODUCTION	1
1.1 Research Background	1
1.2 Problem Statements	4
1.3 Research Objectives	8
1.4 Scopes of Work	8
1.5 Research Methodology	9
1.6 Thesis Contributions	10
1.7 Thesis Outlines	11
2. LITERATURE REVIEW	13
2.1 Introduction	13
2.2 Principle of DTC of Induction Motor Drives	13
2.2.1 Three-Phase Voltage Source Inverter (VSI)	14
2.2.2 Control of Stator Flux	15
2.2.3 Control of Torque	18
2.2.4 Estimation of Stator Flux and Torque	21
2.2.5 Structure of Conventional DTC Drives	23
2.3 Major Problem of Conventional DTC Drives	24
2.4 Performance Improvements of DTC Drives	26
2.4.1 DTC Drives using Carrier Based Modulation	26
2.4.2 DTC using Space Vector Modulation (DTC-SVM)	29
2.4.3 Application of Multilevel Inverter	34
2.5 Summary	41
3. RESEARCH METHODOLOGY	43
3.1 Introduction	43
3.2 Modelling of Induction Motor	44
3.3 Mapping of Voltage Vectors Produced by Three-Level NPC Inverter	48
3.3.1 Three-Level Neutral Point Clamped (NPC) Inverter	49
3.3.2 Space Voltage Vector	51
3.3.3 Voltage Vectors of Three-Level NPC on $d - q$ Voltage Vector Plane	52

3.4	Proposed Strategy	54
3.4.1	Analysis of Torque Slope	55
3.4.2	Proposed Constant Switching Frequency (CSF) Torque Controller of Three-Level NPC Inverter	65
3.4.2.1	Principle of Proposed CSF Torque Controller	65
3.4.2.2	Design of Proposed CSF Torque Controller	69
3.4.2.3	Parameters of Induction Motor and CSF Torque Controller for Various Speed Operation	76
3.4.3	Balancing Control Strategy of NPC Multilevel Inverter	78
3.4.4	Definition of Two Flux Sectors	80
3.4.5	Look-up Table	81
3.5	Proposed DTC Drives Control Structure	83
3.6	Summary	84
4.	SIMULATION AND EXPERIMENTAL SET UP	86
4.1	Introduction	86
4.2	Simulation Model of Proposed DTC Control of Induction Motor	86
4.2.1	Three-Phase Induction Motor	87
4.2.2	Calculation of Stator Voltage Components	90
4.2.3	Calculation of Stator Current Components	90
4.2.4	Estimations of Stator Flux and Electromagnetic Torque	91
4.2.5	Detection of Flux Sectors	92
4.2.6	Torque Proposed Controller	93
4.2.7	Balancing Control Strategy	94
4.2.8	Look-up Table for Selecting Voltage Vectors	95
4.2.9	Three-Level NPC Inverter	96
4.3	Description of Experimental Setup	97
4.3.1	dSPACE DSP DS1104 R&D Controller Board	99
4.3.2	Field-Programmable Gate Array (FPGA) Board	100
4.3.3	Current and Voltage Sensor	101
4.3.4	Gate Driver	102
4.3.5	Power Circuit or Voltage Source Inverter	103
4.3.6	Induction Motor	103
4.4	Summary	104
5.	RESULT AND DISCUSSION	105
5.1	Introduction	105
5.2	Minimization of Switching Frequency	105
5.3	Constant Switching Frequency Operation	114
5.4	Reduction of Torque Ripple	118
5.5	Effect of Small and Large Restriction Error towards DTC drives	128
5.6	Summary	129
6.	CONCLUSION AND RECOMMENDATIONS	131
6.1	Conclusion	131
6.2	Recommendations	132
	REFERENCES	134
	APPENDICES	147

LIST OF TABLES

TABLE	TITLE	PAGE
1.1	Type of Switching State of Short Amplitude of Voltage Vectors and its Effect Toward Capacitor Voltage	6
2.1	Selection of Voltage Vector Tabulated in Look-up Table	24
2.2	Advantages of Multilevel Inverter Compared with Two-Level Inverter	36
3.1	Switching Status and Phase Voltage for Each Leg/Phase of NPC Inverter	50
3.2	Classification of Voltage Vector of Three-Level NPC Inverter	54
3.3	Selection of Voltage Vectors at Different Speed Operation of Conventional DTC	64
3.4	Selection of Voltage Vectors at Different Speed Operation of Proposed Strategy	64
3.5	Parameters of Three-Phase Induction Motor	77
3.6	Parameters of CSF Torque Controller for Low, Medium and High Speed Operation	77
3.7	Look-up Table of Three-Level NPC with Capacitor Voltage Balancing Strategy	82
3.8	Comparison between Conventional DTC, DTC-NPC-HTC and	85

	DTC-NPC-CSF	
5.1	Switching Frequency for Different Torque and Flux Hysteresis Bandwidths at Low Speed Operation (300RPM) for (a) Conventional DTC and (b) DTC-NPC-HTC	107
5.2	Switching Frequency for Different Torque and Flux Hysteresis Bandwidths at Medium Speed Operation (650RPM) for (a) Conventional DTC and (b) DTC-NPC-HTC	108
5.3	Switching Frequency for Different Torque and Flux Hysteresis Bandwidths at High Speed Operation (1000RPM) for (a) Conventional DTC and (b) DTC-NPC-HTC	109
5.4	Value of Switching Frequency and Percentage Reduction of Switching Frequency for Different Speed Operation	110
5.5	Summarization of Torque Ripple Obtained in Conventional DTC and DTC-NPC-HTC for Different Speed Operation Based on Simulation Results	120
5.6	Summarization of Torque Ripple Obtained in Conventional DTC, DTC-NPC-HTC and DTC-NPC-CSF for Different Speed Operation Based on Experimental Results	121

LIST OF FIGURES

FIGURE	TITLE	PAGE
1.1	Structure of FOC of Induction Motor Drives	2
1.2	Structure of DTC of Induction Motor Drives	3
1.3	Problem of Large Torque Ripple and Variable Switching Frequency in Conventional DTC Drives	5
1.4	Imbalance of Capacitor Voltage due to Application of Short Amplitude of Voltage Vectors (i.e. $\bar{v}_{s,S6}$) for Switching State (a) POP (b) ONO	7
2.1	Three-Phase VSI Circuit	14
2.2	Voltage Vectors of Three-Phase VSI	15
2.3	Two-Level Flux Hysteresis Comparator	16
2.4	Typical Waveform of Stator Flux, Flux Error and Flux Error Status for Two-Level Hysteresis Comparator	16
2.5	Selection of Suitable Two Active Voltage Vectors for Each Sectors to Control the Flux within its Hysteresis Band	18
2.6	Three-Level Torque Hysteresis Comparator	19
2.7	Typical Waveforms of Torque, Torque Error and Torque Error Status of Three-Level Hysteresis Comparator	20
2.8	Variation of θ_{sr} with Application of (a) Active Forward Voltage Vectors, (b) Zero Voltage Vectors, (c) Active Reverse	22

	Voltage Vectors	
2.9	Structure of DTC of Induction Motor Drives	23
2.10	Large Torque Ripple in Conventional DTC Drives	25
2.11	Structure of Dithering Technique Implemented to Conventional DTC as Proposed in (Noguchi, Yamamoto, Kondo & Takahashi, 1999)	27
2.12	Structure of a New Switching Strategy with Proposed Torque Controller (Idris & Yatim, 2000)	28
2.13	Structure of New Torque and Flux Controller as Proposed in (Toh, Idris & Yatim, 2003)	29
2.14	Waveform of Torque Ripple Produced by (a) Conventional DTC (b) DTC-SVM	30
2.15	Structure of DTC-SVM Approach (a) DTC-SVM with Closed Flux Control (b) DTC-SVM with Closed-Loop Torque Control (c) DTC-SVM Operated in Polar Coordinates (d) DTC-SVM Operated in Cartesian Coordinates (Stator Flux Oriented Control)	32
2.16	Structure of DTC-SVM (as Proposed in (Lascu, Boldea & Blaabjerg, 2000)	34
2.17	Type of Multilevel Inverter (Three-Level) (a) CHMI (b) FC (c) NPC	35
2.18	Sector I of Space Vector in $\alpha - \beta$ plane with Four Sub-Sectors	39
2.19	Sector I of Space Vector in $\alpha - \beta$ plane with Five Sub-Sectors and Virtual Vector	40
3.1	Cross-section of Single Pole-Pair Three-Phase Induction Motor	45

3.2	Dynamic d - q Equivalent Circuits of Three-Phase Induction Motor (a) d -axis (b) q -axis	47
3.3	Structure of Three-Level of NPC Multilevel Inverter	49
3.4	Space Voltage Vector on d - q Axis Component of Voltage Vector Plane	52
3.5	Voltage Vectors of Three-Level NPC Multilevel Inverter	53
3.6	Control of Torque using Proposed Method (Dotted Line) and the Conventional DTC (Solid Line) at Low Speed Operations (a) Torque Waveforms (b) Torque Error Status	59
3.7	Control of Torque using Proposed Method (Dotted Line) and the Conventional DTC (Solid Line) at Medium Speed Operations (a) Torque Waveforms (b) Torque Error Status	61
3.8	Control of Torque using Proposed Method (Dotted Line) and the Conventional DTC (Solid Line) at High Speed Operations (a) Torque Waveforms (b) Torque Error Status	63
3.9	A Proposed CSF Torque Controller for DTC with Three-Level NPC Inverter	66
3.10	Structure of PI Controller	66
3.11	Torque Error Status of Proposed Method (σ_{CSF}) according to Condition of T_{PI} and Triangular Carrier Waveform	68
3.12	Triangular Carrier Waveform for Proposed Method	70
3.13	Imbalance of Capacitor Voltage When P-type of Short Amplitude of Voltage Vector is Applied	78
3.14	Imbalance of Capacitor Voltage When N-Type of Short	79

	Amplitude of Voltage Vector is Employed	
3.15	Capacitor Voltage Balancing Strategy using Hysteresis Controllers	80
3.16	Definition of Flux Sector for (a) Long and Short Amplitude of Voltage Vector (b) Medium Amplitude of Voltage Vector	81
3.17	Proposed Structure of DTC of Induction Motor Drives utilizing Three-Level NPC Multilevel Inverter with CSF Torque Controller and Balancing Control Strategy	83
4.1	Simulation Model of Control Strategy of DTC of Induction Motor Drives with NPC Inverter	88
4.2	Simulation Model of Three-Phase Induction Motor (<i>Induction Motor</i> in Figure 4.1)	89
4.3	Calculation of Stator Voltage Components (<i>Calculation of Stator Voltage</i> in Figure 4.1)	90
4.4	Calculation of Stator Current Components (<i>Calculation of Stator Current</i> in Figure 4.1)	91
4.5	Estimation of Stator Flux and Electromagnetic Torque (<i>Flux and Torque Estimators</i> in Figure 4.1)	91
4.6	Flowchart of Detection of Flux Sectors (<i>Sector Detection</i> block in Figure 4.1)	93
4.7	CSF torque controller (<i>TPC</i> in Figure 4.1)	94
4.8	Balancing Control Strategy of Three-Level NPC Inverter (<i>Balancing Strategy</i> block in Figure 4.1)	95
4.9	Simulation Model of Three-Level NPC Inverter (<i>3-Level NPC</i>	96

	block in Figure 4.1)	
4.10	Experimental Set Up (a) Block Diagram (b) Actual Platform	98
4.11	FPGA Deo-Nano Controller Board	101
4.12	Current Sensor Implemented on the Hardware Set Up	101
4.13	Voltage Sensor Implemented on the Hardware Set Up	102
4.14	Gate Driver	103
4.15	Power Circuit of Experimentation Set Up for Three-Level NPC Inverter	103
4.16	Three-Phase Induction Motor Connected to DC Generator and Resistive Load	104
5.1	Switching Frequency for Different Hysteresis Bandwidths at Low Speed Operation for (a) Conventional DTC and (b) DTC- NPC-HTC	111
5.2	Switching Frequency for Different Hysteresis Bandwidths at Medium Speed Operation for (a) Conventional DTC and (b) DTC-NPC-HTC	112
5.3	Switching Frequency for Different Hysteresis Bandwidths at High Speed Operation for (a) Conventional DTC and (b) DTC- NPC-HTC	113
5.4	Experimental Result of FFT of Switching Frequency for (a) Conventional DTC (b) DTC-NPC-HTC and (c) DTC-NPC- CSF at Low Speed Operation	115
5.5	Experimental Result of FFT of Switching Frequency for (a) Conventional DTC (b) DTC-NPC-HTC and (c) DTC-NPC-	116

	CSF at Medium Speed Operation	
5.6	Experimental Result of FFT of Switching Frequency for (a) Conventional DTC (b) DTC-NPC-HTC and (c) DTC-NPC- CSF at High Speed Operation	117
5.7	Illustration of Torque Graph for Calculation of Torque Ripple Percentage	120
5.8	Simulation Results of Torque Ripple Reduction for (a) Conventional DTC and (b) DTC-NPC-HTC at Low Speed Operation	122
5.9	Simulation Results of Torque Ripple Reduction for (a) Conventional DTC and (b) DTC-NPC-HTC at Medium Speed Operation	123
5.10	Simulation Results of Torque Ripple Reduction for (a) Conventional DTC and (b) DTC-NPC-HTC at High Speed Operation	124
5.11	Experimental Results of Torque Ripple Reduction for (a) Conventional DTC (b) DTC-NPC-HTC and (c) DTC-NPC- CSF at Low Speed Operation	125
5.12	Experimental Results of Torque Ripple Reduction for (a) Conventional DTC (b) DTC-NPC-HTC and (c) DTC-NPC- CSF at Medium Speed Operation	126
5.13	Experimental Results of Torque Ripple Reduction for (a) Conventional DTC (b) DTC-NPC-HTC and (c) DTC-NPC- CSF at High Speed Operation	127

5.14	Experimental Results of Torque (T_e), Stator Flux (ψ_s), Phase Voltage (V_{an}) and Error of Capacitor Voltage (ε_v) for restriction error of $\pm 2V$ (left) and $\pm 15V$ (right)	129
------	--	-----

LIST OF APPENDICES

APPENDIX	TITLE	PAGE
A	Derivation of torque equation in term of stator and rotor flux	147
B	The derivation of angular frequency of stator flux	148
C	The averaging and linearization of torque equations	149
D	Matlab source coding listing to determine the proportional and integral gain for low, medium and high speed operation (K_{pL} , K_{iL} , K_{pM} , K_{iM} , K_{pH} and K_{iH})	151
E	Matlab source coding listing	154
F	VHDL source coding listing	160

LIST OF ABBREVIATIONS

AC	- Alternating Current
ADC	- Analog to digital converter
B	- Viscous friction
CHMI	- Cascaded H-Bridge Multilevel Inverter
CSF	- Constant Switching Frequency
DAC	- Digital to analogue converter
DC	- Direct current
DSP	- Digital Signal Processor
DT	- Sampling Time
DTC	- Direct Torque Control
DTC-NPC-CSF	- Referred to DTC using NPC with Proposed Constant Switching Frequency Torque Controller
DTC-NPC-HTC	- Referred to DTC utilizing NPC with Hysteresis Torque Controller
DTC-SVM	- Direct Torque Control using Space Vector Modulation
FC	- Flying Capacitor
FOC	- Field Oriented Control
FPGA	- Field Programmable Gate Arrays
IGBT	- Insulated Gate Bipolar Transistor
IM	- Induction Motor

J	-	Moment of inertia
LB	-	Lower Band
MB	-	Middle Band
NP	-	A point between two capacitors or neutral point
NPC	-	Neutral Point Clamped
P	-	Number of pole pairs
PI	-	Proportional-Integral
SVM	-	Space Vector Modulated
UB	-	Upper Band
VHDL	-	VHSIC hardware description language
VSI	-	Voltage Source Inverter
VSC	-	Variable-Structure Control
$C_{pp,H}$		Peak-to-peak carrier for high speed
$C_{pp,M}$		Peak-to-peak carrier for medium speed
$C_{pp,L}$		Peak-to-peak carrier for low speed
C_{upper}, C_{lower}	-	Upper and lower carrier triangular waveform
d, q	-	Direct and quadrature of the stationary reference frame
d^r, q^r	-	Real and imaginary and real of the rotor
f	-	Frequency
HB_{ψ}	-	Flux hysteresis bandwidth
HB_{T_e}	-	Torque hysteresis bandwidth
\bar{i}_s, \bar{i}_r	-	Stator and rotor current vector
i_a, i_b, i_c		Current of phase a. b and c
i_{sd}, i_{sq}	-	Real and imaginary stator current in stationary reference frame

i_{rd}, i_{rq}	- Real and imaginary rotor current in stationary reference frame
K_p	- Proportional gain
K_i	- Integral gain
N_c	- Number of commutation of switching state
N_s	- Number of Sample
L_m	- Mutual self-inductance
L_s, L_r	- Stator and rotor self-inductance
L_{ls}, L_{lr}	- Stator and rotor leakage-inductance
R_s, R_r	- Stator and rotor resistance
S_a, S_b, S_c	- Upper switching state of phase a, b and c
$\overline{S}_a, \overline{S}_b, \overline{S}_c$	- Lower switching state of phase a, b and c
S_f	- Switching Frequency
T_{ave}	- Average torque
$T_{e,ref}$	- Reference of electromagnetic torque
T_e	- Electromagnetic torque
T_{load}	- Torque load
T_{max}	- Maximum of torque
T_{min}	- Minimum of torque
T_{pi}	- Torque error from PI controller
T_r	- Torque ripple reduction
V_{dc}	- DC voltages
\bar{v}_s	- Voltage vectors
v_{c1}, v_{c2}	- Upper and lower capacitor voltage
v_{an}, v_{bn}, v_{cn}	- Phase voltage of stator winding using two-level inverter

v_{sd}, v_{sq}	- Real and imaginary stator voltage in stationary reference frame
$v_{sd,ref}, v_{sq,ref}$	- Reference of real and imaginary stator voltage in stationary reference frame
\bar{x}	- Referred to voltage or current or flux linkage
$\psi_{s,ref}$	- Reference of flux
ψ_s	- Estimated of flux
$\bar{\psi}_s, \bar{\psi}_r$	- Stator and rotor flux linkage space vector in stationary reference frame
ψ_{sd}, ψ_{sq}	- Real and imaginary stator flux linkage in stationary reference frame
σ	- Total flux leakage factor ($\sigma = 1 - L_m^2/L_s L_r$)
σ_B	- Balancing status
σ_{CSF}	- Torque error status from CSF torque controller
σ_ψ	- Flux error status
σ_τ	- Torque error status for conventional DTC
ε_ψ	- Flux error
ε_τ	- Torque error
ω	- Steady state synchronous frequency in rad/s
ω_r	- Rotor electrical speed in rad/s
ω_m	- Mechanical angular speed in rad/s
θ_f	- Field angle
θ_{sr}	- Load angle or angle between stator flux and rotor flux linkage
θ^s	- The angle between d axis and \bar{x}
θ^r	- The angle between d^r axis and \bar{x}